INTERNATIONAL SOCIETY FOR
SOIL MECHANICS AND
GEOTECHNICAL ENGINEERING

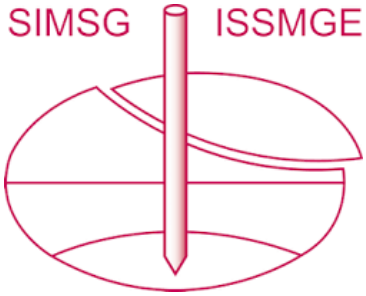

This paper was downloaded from the Online Library of the International Society for Soil Mechanics and Geotechnical Engineering (ISSMGE). The library is available here:

https://www.issmge.org/publications/online-library

This is an open-access database that archives thousands of papers published under the Auspices of the ISSMGE and maintained by the Innovation and Development Committee of ISSMGE.

Failure by large plastic deformations

Rupture par grande déformation plastique

R. J. TERMAAT, Ministry of Public Works, The Hague, Netherlands
P. A. VERMEER, Delft University of Technology, Delft, Netherlands
G. J. H. VERGEER, Ministry of Public Works, The Hague, Netherlands

SYNOPSIS The instabilities that occurred during the construction of a closure dam are evaluated by three methods, namely slip-surface analysis, the method of characteristics and an elastoplastic finite element computation. The field observations indicate failure by large plastic deformation of the soft subsoil. The results of the finite element computation confirm the importance of the large undrained deformations. Data on the shear strength and the shear modulus is systematically compared to data from other studies.

INTRODUCTION

In 1976 the Dutch government decided to close the Oosterschelde estuary in the south-west part of the Netherlands with a storm-surge barrier in combination with a number of secondary dams. One of these secondary dams is the Markiezaatsdam. During the construction of this 4 km long dam several instabilities occurred.

To use this experience for the construction of the second secondary dam (Oesterdam), an extensive study of the mechanism of those instabilities has been performed. In this study different theories have been used, not only the conventional stability analysis with circular slip surfaces, but also the method of characteristics and an advanced finite element method.

The outcome of the theoretical analyses and the field observations indicate failure by large plastic deformation of the soft clay and peat subsoil. Even slip-circle analyses indicate the importance of large plastic deformations, as a large group of near-critical slip surfaces is found.

This paper presents the main results of the study for the most important cross-section of the dam.

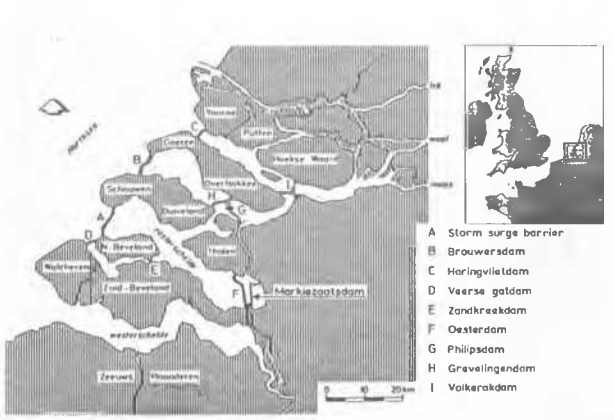

Fig. 1. Location of the Markiezaatsdam

CONSTRUCTION

The geometry shortly before failure is given in Fig. 2.

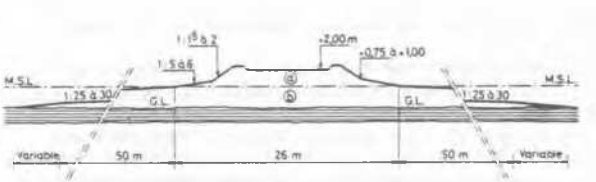

Fig. 2. Geometry shortly before failure.

First a sill of sand was built by hydraulic fill to mean sea level (MSL); layer b in Fig. 2. Because no surrounding dikes of stony material were used, the slope of the sill varied from 1:25 to 1:30. For the actual dam (above MSL) a steeper slope was constructed by using bunds of sand. The instabilities occurred, when the embankment reached a level of about 2 m + MSL. Using equipment of a high capacity, the sill and the dam were constructed in a period of two weeks, so that the situation can be considered as undrained.

OBSERVED INSTABILITIES

The instabilities occurred at the moment that the dam had a level of about 2.00 m + MSL. The dam failed by sinking over a part or over the entire crest width, whilst the adjacent sill slightly rose. Before failure cracks developed at the surface of the sand sill, which widened after the failure. The cracks were parallel to the length axis of the dam. About 4 or 5 days after the first instability a dark strip of blue soft clay could be seen on the edge of the sand sill.

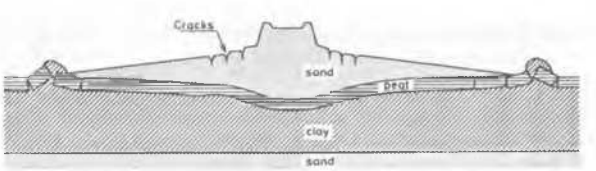

Fig. 3. Cross-section of the dam after failure.

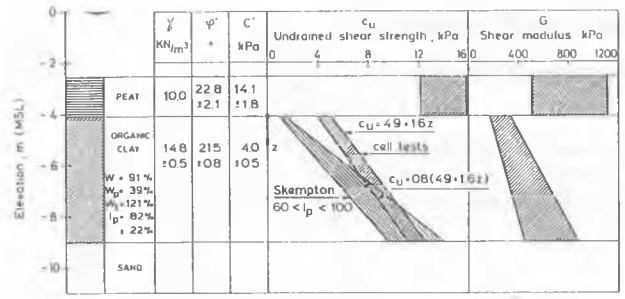

Fig. 4. Soil properties

SOIL PROPERTIES

The subsoil consists of peat, soft clay and deep sand as indicated in the Figs. 3 and 4. For the stability, the relatively thick clay layer is considered most dominant. Hence, special attention was given to the shear strength of the clay. The effective strength parameters (φ' and c') were evaluated from the results of 15 Dutch cell tests [3] . These data may be used to calculate the undrained shear strength c_u (or s_u). We used the formula

$$c_u = c' \cos \varphi' + 1/2 \, (\sigma_v' + \sigma_h') \sin \varphi'$$

where σ_v' and σ_h' are initial stresses and we used $\sigma_h' = 0.6 \, \sigma_v'$

In order to check the reliability of the above c_u -evaluation, we may consider Skempton's empirical relation between the ratio of c_u / σ_v' and the plasticity index I_p (or PI). The data in Fig. 4. show that our c_u-evaluation compares well to Skempton's rule. We obtain a range of possible c_u-values rather than a unique value as a function of the depth, as the Markiezaats clay has a plasticity index in the range $60 < I_p < 100$%. Skempton's rule is plotted in Fig. 5. and his data for various clays are extended by data from some other researchers. We also added results from triaxial tests being performed for another dam in the estuary. Fig. 5. gives confidence in Skempton's rule. Fig. 4. shows that our evaluation gives more or less similar values.

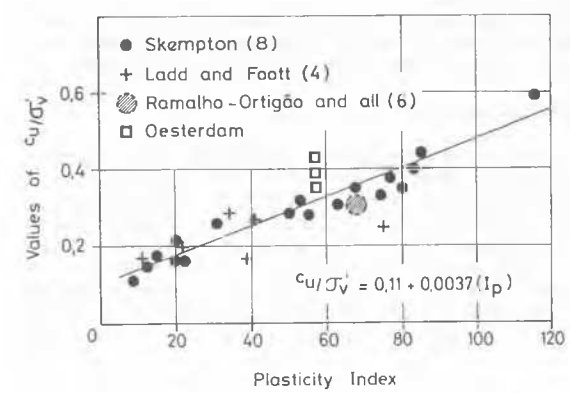

Fig. 5. Skempton's relationship between c_u, σ_v' and I_p for normally consolidated clay.

No tests were performed to determine the undrained shear modulus (G) of the clay. Therefore data has been used from Foott and Ladd [2] and results from triaxial and pressiometer tests performed for the Oesterdam, as plotted in Fig. 6. For the Markiezaats clay with $60 < I_p < 100$ this figure indicates the shear modulus-shear strength range $40 < G/c_u < 75$.

The strength properties of the peat were again determined from cell tests. For the undrained shear modulus, we used the same ratio between G and c_u as for the clay.

Th properties of the sand are based on experience. In the calculations we used G= 20.000 kPa, $\varphi' = 30°$ and $c' = 0$.

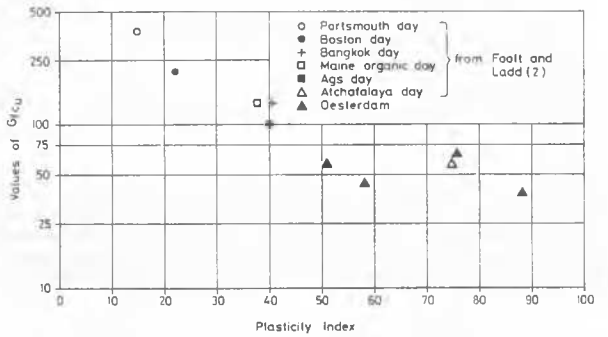

Fig. 6. Relationship between G, c_u and Ip for normally consolidated clays; G is taken at 50% strength.

ANALYSIS WITH SLIP SURFACES

In the calculations the clay-strength was assumed to increase linearly with depth according to the equation $c_u = \alpha (4.9 + 1.6z)$. The contributions of the sand sill and the peat layer to the bearing capacity of the subsoil were conveniently neglected. Then, the factor of safety becomes proportional to the α-factor for c_u, giving a straight line in Fig. 7. The range for $0.8 < \alpha < 1$ is particularly important as it covers precisely the c_u- values as evaluated from the Dutch cell tests. Here, we find safety factors slightly beyond unity. At first look a low value near unity seems to be not very worrying as:

- the schematization is on the safe side, a.o. due to neglect of the strong peat layer and the sand sill
- strength data from cell tests are generally on the safe side as the test procedure limits the deformation
- we consider a construction stage for which collapse has no dramatic consequences.

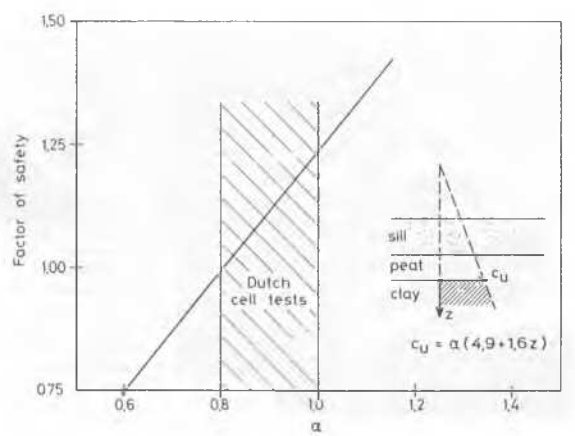

Fig. 7. Relationship between factor of safety and undrained shear strength of the clay, when neglecting the resistance of the sill and peat.

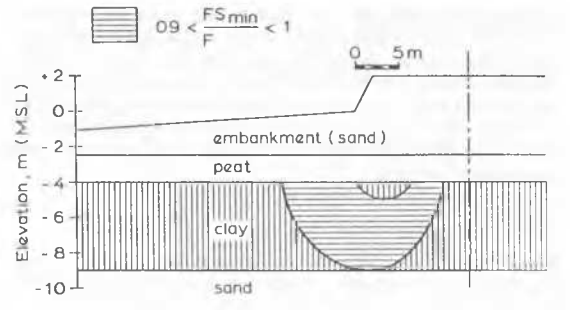

Fig. 8. Area's with equal factor of safety based on slip circle analysis.

However, these analyses do not account for the deformations of the subsoil and the resulting settlements. An indication for the occurrence of large deformations is obtained by considering the safety factors for many slip surfaces rather than only the critical slip surface. Many slip surfaces appear to be near critical, covering a part of the clay layer as plotted in Fig. 8. In fact, a region of the subsoil is near failure and consequently intensively deformed.

METHOD OF CHARACTERISTICS

Matar and Salençon [5] have derived formulas that satisfy both the kinematic and equilibrium conditions. Basicly those formulas have been established from the determination of the bearing capacity of a rigid foundation on a cohesive subsoil. Silvestri [7] showed that the method of characteristics can also be applied to embankments. From the paper by Matar and Salençon we obtained the following equation for the ultimate stress P at a cohesive layer:

$$P = Po + 4{,}14\ \mu C' + \mu\left(\frac{\lambda}{d}\ C^{\circ} + g^{\circ}\right)x$$

C° = shear strenght at the top of the soft layer

μ = coëfficient which expresses the form of the characteristics field as a function of the ratio b/d (see Fig. 9.); $\mu = 1.35$

λ = factor which represents the relative mobilisation of the shear strenght at the two interfaces at the top and at the bottom of the soft clay layer, for λ the value 2 has been chosen (perfectly rough contacts)

g° = gradient of the shear strenght in the cohesive layer

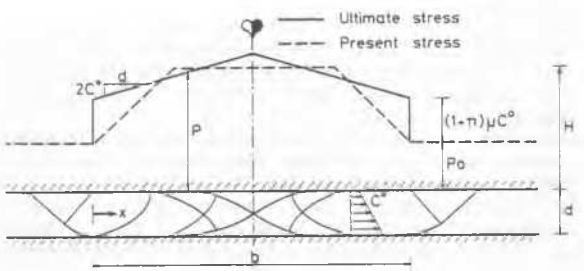

Fig. 9. Solution Matar en Salençon.

When using the approach we obtained a larger safety factor than previously calculated by means of the slip-circle analysis.

FINITE ELEMENT COMPUTATIONS

From the idea that deformation and stability of soft clay are highly correlated, a finite element model with an elasto-plastic stress-strain relation has been applied. The power of elasto-plastic computation is that it is a coupled approach to deformation and stability.

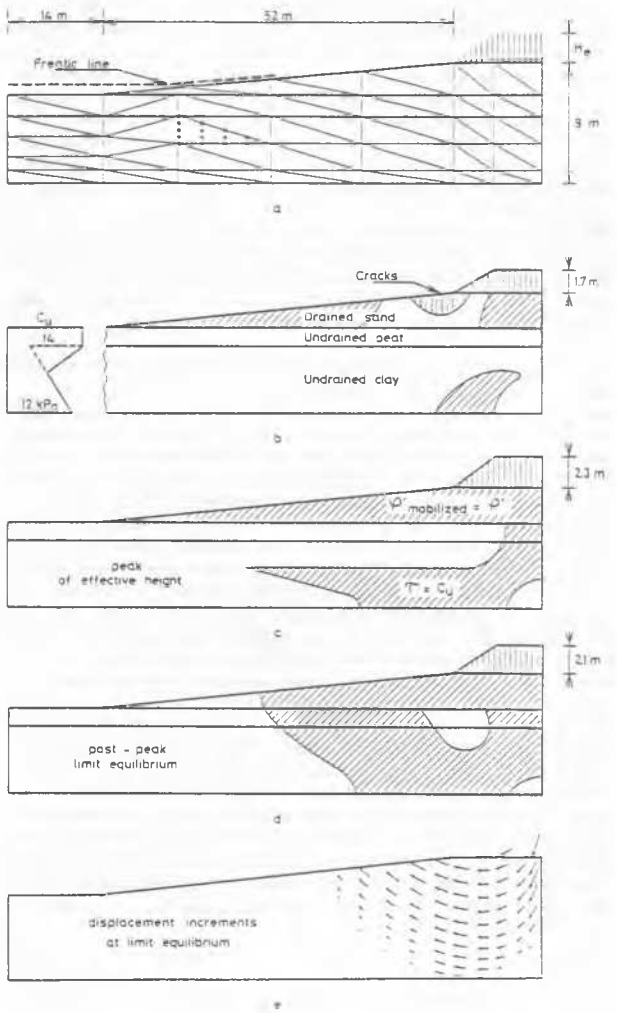

Fig. 10. Finite element mesh, development of plastic zones (shaded) and ultimate failure mechanism. Note the scale distortion.

We used 15-noded triangular elements as shown in Fig. 10 [1].
The undrained shear strenght for use in the computation are given in Fig.10b at least for the soft soil. The dashed line which derives from the theoretical equation is adjusted as a gradual transition from the peat to the clay seems to be more realistic. The shear modules for the soft soil was taken to be $G=75\ c_u$ and a Poisson's ration of 0.49 was used to simulate incompressibility. The total stress analysis for undrained behaviour did not apply to the sand sill. Here, the pore pressures are hydrostatic with a sloping freatic line partly along the surface. Pore pressures and effective stresses were added in the equilibrium equations.

The shear modulus of the sand and the Poisson's ratio were estimated to be 20000 kN/m^2 and 0.3 respectively; the effective strenght parameters are c'=0 and φ'=30°.

The computation proceeds in two stages. First the stresses due to the weight of the sill are computed. Then, the construction of the dam is simulated by augmenting external loads on top of the sill, which is initially at mean sea level. This gives the dashed line in Fig.11, for which we actually used a considerable number of small load increments with equilibrium iterations. The dashed curve gives the load or rather the height of the fill that is felt by the subsoil. The effective height above mean sea level is the height of the fill minus the settlement of the sill. Subtracting the computed settlements from the dashed curve we obtain the bold curve in Fig.11, with a peak value of 2.3 m for the effective height. In the unstable post-peak regime, the settlements simply exceed the speed of construction.
According to the calculations, a plastic zone develops very soon in the relatively stiff sill (Fig.10b). Then the deep clay becomes more and more plastic and this gives the strong non-linearily in Fig.11. Finally, the strong peat layer becomes plastic.

The computational results predict a very abrupt settlement at an effective height of 2.3 m. In fact, an abrupt settlement was observed at 2.0 m., so that the stiffness of the peat and/or clay is slighly overestimated. Let us assume that we have overestimated the stiffness of all soil layers to the same degree. Then, the best-fit shear modulus is computable from the present results, as a change of the shear modulus only involves a distortion of the settlement scale in Fig.11. The best-fit shear modulus is G=40c_u as can be seen from the following. When using G=40c_u instead of G=75c_u, the computed settlement must be multiplied by the factor 75/40, so that we obtain the lower curve in Fig.11 with a peak of 2m. Considering the data in Fig.6 and the plasticity index of the clay we also obtain a shear modulus of about 40 c_u.
The Figs. 10d and 10e relate to the ultimate failure situation well beyond the peak. The plastic zone has fully developed. The contours in Fig. 8 from slip-circle calculations are within this plastic zone. The displacement increments in Fig.11e indicate the occurrence of an almost circular slip surface. The difference with a slip-circle analysis is that we have incorporated the settlements to obtain failure before the limit state of equilibrium is reached.

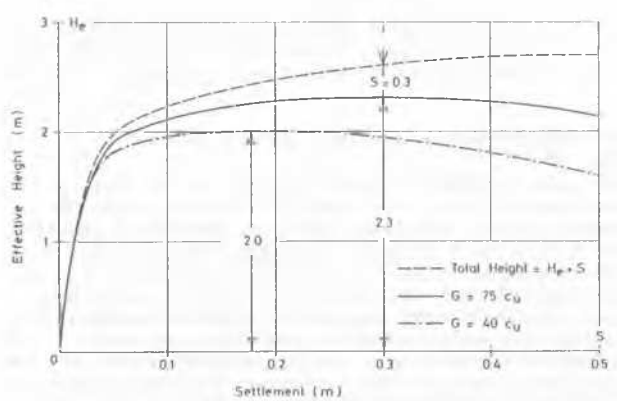

Fig. 11. Computed settlement versus the height of the dam.

When these settlements are neglected a safety factor of about 1.3 would be obtained. This value is found by dividing the limit value of the dashed curve in Fig. 11 by the embankment height of 2 m. A virtually identical value was obtained from a slip-surface analysis [9]. Fig. 7 suggests lower values but those results are based on analyses in which the sand sill and the peat layer are neglected.

CONCLUSION

An observed dam failure was analysed by various theoretical stability methods. Field observations indicate failure by large plastic deformation. The finite element computation confirms this phenomenon.
The finite element method provides detailed information. Good agreement is found for the limit state situation of ultimate equilibrium. The finite element method gives a failure mechanism with a slip surface that is almost identical to the critical circle from the slip-circle analysis. This factor of safety is on the high side, as the deformations give an unstable situation before the limit state of stress is reached. In general, the effect of large deformation is of import for soft subsoil.
When considering deformations, good data is needed on the shear moduli of the soil layers. A comparison of data, including results from previous studies, shows a clear decrease of the G/c_u ratio with increase of the plasticity index.
The undrained shear strength as derived from Dutch cell-test experiments is in line with Shempton's empirical relationship.

REFERENCES

1. de Borst, R., Vermeer, P.A. (1984). Possibilities and limitations of finite elements for limit analysis. Géotechnique 34, No.2, pp 199-210.
2. Foott, R., Ladd, C.C. (1981). Undrained settlement of plastic and organic clays, Journ.Geot.Div., ASCE, No.GT8., pp 1079-1094.
3. Heynen, W.J., van Duren, F.J. (1979). The Dutch cell test; comparison of results of cell tests and triaxial tests on clay, Proc. VII ECSMFE, Brighton U.K., volume 2, pp. 157-161.
4. Ladd, C.C., Foott, R. (1974). New design procedure for stability of soft clays, Journ.Geot. Div., ASCE No.GT7, pp 763-786.
5. Matar, M., Salençon, J. (1977). Capacité portante d'une semelle filante sur sol purement cohérent d'épaisseur limitée et de cohesion variable avec la profondeur, Ann. de l'Inst. Techn. du Batt. des Traveaux Publics, No. 352, pp. 93-108.
6. Ramalho-Ortigão, J.A., Mauro, M., Werneck, L.G., Lacerda, W.A. (1983). Embankment failure on clay near Rio de Janeiro, Journ. Geot. Div., ASCE, No. 11.
7. Silvestri, V. (1983). The bearing capacity of dykes and fills founded on soft soils of limited thickness, Canadian Geot. Journ., Volume 20, No.3. pp. 428-436.
8. Skempton, A.W. (1957). Discussion on "the planning and design of the new Hong Kong airport" (Grace and Henry), Proc.Inst.Civil Eng. 7.
9. Ernst, R.J., Vermeer, P.A. (1984). Finite element computation of the Markiezaatsdam (in Dutch), Report No. 230 of the Geot. Lab.,Delft Univ. of Technology.